Metabolic Engineering Communications 3 (2016) 234–244

Contents lists available at ScienceDirect

Metabolic Engineering Communications

journal homepage: www.elsevier.com/locate/mec

Creating metabolic demand as an engineering strategy in *Pseudomonas putida* – Rhamnolipid synthesis as an example

Till Tiso [a], Petra Sabelhaus [a], Beate Behrens [b], Andreas Wittgens [c], Frank Rosenau [c], Heiko Hayen [b], Lars Mathias Blank [a,*]

[a] iAMB – Institute of Applied Microbiology, ABBt – Aachen Biology and Biotechnology, RWTH Aachen University, Worringerweg 1, D-52074 Aachen, Germany
[b] Institute of Inorganic and Analytical Chemistry, University of Münster, Corrensstraße 30, D-48149 Münster, Germany
[c] Ulm Center for Peptide Pharmaceuticals, Ulm University, Albert-Einstein-Allee 11, D-89081 Ulm, Germany

ARTICLE INFO

Article history:
Received 7 October 2015
Received in revised form
19 July 2016
Accepted 6 August 2016
Available online 8 August 2016

Keywords:
Metabolic control
Rhamnolipid
Non-pathogenic Pseudomonas
Biosurfactant
Driven by demand
Synthetic promoter

ABSTRACT

Metabolic engineering of microbial cell factories for the production of heterologous secondary metabolites implicitly relies on the intensification of intracellular flux directed toward the product of choice. Apart from reactions following peripheral pathways, enzymes of the central carbon metabolism are usually targeted for the enhancement of precursor supply. In *Pseudomonas putida*, a Gram-negative soil bacterium, central carbon metabolism, i.e., the reactions required for the synthesis of all 12 biomass precursors, was shown to be regulated at the metabolic level and not at the transcriptional level. The bacterium's central carbon metabolism appears to be driven by demand to react rapidly to ever-changing environmental conditions. In contrast, peripheral pathways that are only required for growth under certain conditions are regulated transcriptionally. In this work, we show that this regulation regime can be exploited for metabolic engineering.

We tested this driven-by-demand metabolic engineering strategy using rhamnolipid production as an example. Rhamnolipid synthesis relies on two pathways, i.e., fatty acid *de novo* synthesis and the rhamnose pathway, providing the required precursors hydroxyalkanoyloxy-alkanoic acid (HAA) and activated (dTDP-)rhamnose, respectively. In contrast to single-pathway molecules, rhamnolipid synthesis causes demand for two central carbon metabolism intermediates, i.e., acetyl-CoA for HAA and glucose-6-phosphate for rhamnose synthesis.

Following the above-outlined strategy of driven by demand, a synthetic promoter library was developed to identify the optimal expression of the two essential genes (*rhlAB*) for rhamnolipid synthesis. The best rhamnolipid-synthesizing strain had a yield of 40% rhamnolipids on sugar [$Cmol_{RL}/Cmol_{Glc}$], which is approximately 55% of the theoretical yield. The rate of rhamnolipid synthesis of this strain was also high. Compared to an exponentially growing wild type, the rhamnose pathway increased its flux by 300%, whereas the flux through *de novo* fatty acid synthesis increased by 50%.

We show that the central carbon metabolism of *P. putida* is capable of meeting the metabolic demand generated by engineering transcription in peripheral pathways, thereby enabling a significant rerouting of carbon flux toward the product of interest, in this case, rhamnolipids of industrial interest.

1. Introduction

Our society relies heavily on crude oil and the products derived thereof. To reduce this dependence, sustainable processes based on renewable resources must be established. One such method is whole-cell biocatalysis using sugars as a substrate. A bacterial species with excellent characteristics for this technique is *Pseudomonas putida*, a Gram-negative, saprotrophic soil bacterium with a very versatile metabolism and high tolerance to organic solvents (Ramos et al., 1995). These characteristics have made *P. putida* a much discussed host for industrial applications (Tiso et al., 2015), although only a few examples exist thus far.

Abbreviations: CDW, cell dry weight; LPS, lipopolysaccharide; FBA, flux balance analysis; CCM, central carbon metabolism; PHA, polyhydroxyalkanoate; PP pathway, pentose phosphate pathway; ED pathway, Entner-Doudoroff pathway; RL, rhamnolipid; TCA, tricarboxylic acid; HAA, hydroxyalkanoyloxy-alkanoic acid

* Corresponding author.
E-mail addresses: till.tiso@rwth-aachen.de (T. Tiso), petra.sabelhaus@rwth-aachen.de (P. Sabelhaus), behrensb@uni-muenster.de (B. Behrens), andreas.wittgens@uni-ulm.de (A. Wittgens), frank.rosenau@uni-ulm.de (F. Rosenau), heiko.hayen@uni-muenster.de (H. Hayen), lars.blank@rwth-aachen.de (L.M. Blank).

http://dx.doi.org/10.1016/j.meteno.2016.08.002

Metabolic engineering of secondary metabolite producers implicitly relies on high flux through central carbon metabolism (CCM). This high flux caused by the demand for carbon and energy for the synthesis of the molecule of interest, however, is rarely matched, requiring substantial improvements in CCM operation. The reactions of the CCM are providing the twelve precursors for biomass, i.e., for proteins, nucleic acids, polysaccharides, and lipids (Noor et al., 2010).

An excellent example of rational strain engineering by optimizing the flux distribution and channeling it to the product of choice was reported by Becker et al. (2011). The authors introduced 12 genome-based changes, including the overexpression of five genes encoding for enzymes fueling precursor-synthesizing pathways. In addition, the deletion or down-regulation of two genes encoding enzymes catalyzing competing reactions were introduced, yielding an L-lysine-overproducing strain of *Corynebacterium glutamicum*.

In contrast with this example, we here propose an approach that does not require substantial modifications of the host strain but, rather, relies on the capability of the organism to reroute flux driven by a given (in our case, engineered) demand.

The strategy used here exploits the findings of Koebmann et al., (2002), who observed a strong increase in flux through glycolysis in *Escherichia coli* after introducing an ATP sink, thus discovering the concept of "driven by demand."

It was recently shown that the CCM in *P. putida* is not transcriptionally regulated but, rather, is metabolically regulated (Sudarsan et al., 2014). Despite substantial rerouting of flux during growth on glucose, fructose, and benzoate, the transcription levels of the genes for CCM remain constant. Notably, the carbon substrate degradation pathways beta-ketoadipate and Entner-Doudoroff are transcriptionally regulated (Koebmann et al., 2002). Indeed, there is also evidence from extreme growth conditions (e.g., growth in the presence of a second phase of octanol) that *P. putida* can match metabolic demand by tripling the glucose uptake rate without producing any side products; thus, only biomass and CO_2 are formed by this bacterium (Blank et al., 2008).

An example of this strategy is an engineered *P. putida* that hyper-produces polyhydroxyalkanoate (PHA) (Poblete-Castro et al., 2013). The authors deleted one gene (*gcd*, encoding for glucose dehydrogenase), which led to the rerouting of fluxes to the desired product. They were able to increase PHA accumulation by 100%.

In contrast to these results, peripheral pathways, which are not part of the CCM, are not as easily modified. Establishing a high production rate of aromatics from sugars in *P. putida* again entails substantial modifications to reroute intracellular flux resulting from the regulation of the synthesis pathways of aromatics. This regulation relies on the biosynthesis pathways of specific amino acids, which are regulated allosterically (Wierckx et al., 2005).

To verify the engineering-by-demand approach, we chose rhamnolipid synthesis as an example. It was earlier shown that *P. putida* is able to produce rhamnolipids after introducing two genes of the rhamnolipid synthesis pathway from *P. aeruginosa,* encoding RhlA and RhlB (Wittgens et al., 2011; Ochsner et al., 1994). The demand for precursors (i.e., increased flux through the rhamnose activation pathway and *de novo* lipid synthesis) varied according to the different promoter strengths of the *rhlAB* operon. The flux redistribution is estimated and the results are discussed in the context of the implications of the driven-by-demand concept for constructing superior production strains based on *P. putida*.

2. Materials and methods

2.1. Bacterial strains and culture conditions

The bacterial strains used, *Pseudomonas putida* KT2440 (Nelson et al., 2002) and *Escherichia coli* DH5α (Hanahan, 1983), were routinely cultivated in lysogeny broth (LB) medium (10 g/L tryptone, 5 g/L yeast extract, 10 g/L NaCl) (Bertani, 1951) at 30 °C for *P. putida* and at 37 °C for *E. coli*. Cells containing the vector pVLT31 (de Lorenzo et al., 1993) and its derivatives were selected by adding tetracycline at concentrations of 10 μg/mL for recombinant *E. coli* and 20 μg/mL for *P. putida*. For the selection of pBBR1MCS-3 and derivatives, 20 μg/mL tetracycline was added. Rhamnolipid production by *P. putida* was conducted in LB medium containing 10 g/L glucose and 20 μg/mL tetracycline. The cells were cultivated in a 500 mL shake flask without baffles filled with 50 mL of the cultivation medium and using a MultiTron shaker (INFORS HT Bottmingen, Switzerland) at 250 rpm, with a throw of 25 mm and humidity of 80%.

2.1.1. Isotope labeling experiments

Rhamnolipid-producing *P. putida* KT2440 pPS05 was grown under the conditions stated above. As media, LB medium and M9 minimal medium ($Na_2HPO_4 \times 2H_2O$ 12.8 g/L, KH_2PO_4 3 g/L, NaCl 0.5 g/L, NH_4Cl 1.0 g/L, 2 mM $MgSO_4$ and 2 mL/L US trace elements solution (37% fuming HCl 82.81 mL/L, $FeSO_4 \times 7H_2O$ 4.87 g/L, $CaCl_2 \times 2H_2O$ 4.12 g/L, $MnCl_2 \times 4H_2O$ 1.50 g/L, $ZnSO_4 \times 7H_2O$ 1.87 g/L, H_3BO_3 0.30 g/L, $Na_2MoO_4 \times 2H_2O$ 0.25 g/L, $CuCl_2 \times 2H_2O$ 0.15 g/L, $Na_2EDTA \times 2H_2O$ 0.84 g/L)) (Sambrook et al., 1989) were used. As a carbon source, 10 g/L regular glucose or uniformly isotope-labeled U-$^{13}C_6$ glucose (Cambridge Isotope Laboratories, Inc., Tewksbury, MA, USA) was applied. Tetracycline was added to a final concentration of 20 μg/mL. Samples were obtained twice: once after 8 h and the second after 24 h.

2.2. Expression vectors

For the promoter libraries, degenerated primers (Table 1) were applied carrying the consensus sequences at the −35 and the −10 position of a σ^{70}-promoter (according to Jensen and Hammer (1998)). In this approach (already described in (Beuker et al., 2016)), the two regions of the promoter are conserved, while the remaining nucleotides are randomized. The here used promoter contains 40 nucleotides of which 12 are conserved in the RNA polymerase binding sides, hence 28 nucleotides are degenerated resulting in an high number of possible promoters (4^{28}).

The first fragment carrying the mono-rhamnolipid production genes *rhlAB* and the synthetic promoter were amplified from the *P. aeruginosa* genome using primers Fw-P_{syn}-rhlAB and Rev-P_{syn}-

Table 1
PCR primers used in this work. Underlined letters in the nucleotide sequences mark the restriction sites.

Name	Direction	Used for	Template	Contains	Sequence
Fw-P_{syn}-rhlAB	fwd	pSynProXX	pBBR1	SgsI, SynPro	AAAAAGGCGCGCC(N)$_5$TTGACA(N)$_{17}$TATAAT(N)$_6$
					CATCGGCTACGCGTGAACACGGACGCCAATCGTTTGC
Rev-P_{syn}-rhlAB	rev	pSynProXX	pBBR1		TCAGGACGCAGCCTTCAGCCATCGAGCATCC

rhlAB. The used vector backbone was pBBR1MSC-3, a broad host range plasmid, which encodes for tetracycline resistance (Kovach et al., 1995). After restriction and ligation of fragment and vector, the plasmids were transformed into *E. coli* DH5α. The appearing colonies were washed from the selective plate and the plasmid DNA was isolated. This plasmid mixture was again transformed, this time into *P. putida* KT2440. A first screening was carried out using selective blood agar plates, which were examined regarding hemolytic activity. The construct that showed the highest titer was named pSynPro8 (Wittgens, 2013).

However, this plasmid contained two identical terminator sequences and the native upstream region of *rhlA* from *P. aeruginosa* (a 228 bp-long DNA sequence). This region was removed, and the terminator upstream of the promoter was exchanged. A synthetic DNA fragment was designed and subsequently synthesized by IDT (Integrated DNA Technologies, Inc., Coralville, IA, USA) with the terminator sequence T_0 of a *rho*-independent transcriptional terminator of phage lambda (Silva-Rocha et al., 2013):

5′**AGATCT**CTTGGACTCCTGTTGATAGATCCAGTAATGACCTCAGAACTCCATCTG
GATTTGTTCAGAACGCTCGGTTGCCGCCGGGCGTTTTTTATTGGTGAGAATCCAG
GGTACCTTGACAAAGCGCTTACCTCTTTCTATAATATAGAG**CGTACG**AGGGGGT
TCTAGAGATG 3′.

The 5′ and 3′ regions were complementary to the vector backbone and were used for insertion. Between these regions, the new terminator sequence T_0 (underlined) was introduced. This sequence was exchangeable through the two restriction sites: 5′ BglII AGATCT and 3′ KpnI GGTACC (restriction sites are marked with bold letters). Other exchangeable elements were the promoter (small dots) with 5′ KpnI and 3′ BsiWI CGTACG. The promoter was a synthetic promoter originating from the above-mentioned promoter library. In addition, we introduced a ribosome biding site (large dots), which is exchangeable with the restriction enzymes 5′ BsiWI CGTACG and 3′ XbaI TCTAGA. The transcription start was at the 3′ end (broken line).

Between the promoter and the transcription start, the ribosomal binding site sequence AGGGGG was introduced because this sequence was determined by thermodynamic calculations to lead to particularly strong translation (Rühl, 2012). The distance to the start codon was chosen to be eight base pairs and included a restriction site. All of the elements were exchangeable via single cutter restriction sites. The plasmid was digested with PciI and BglII, and Gibson Assembly was used for combining of the synthetic DNA fragment with the vector backbone. The new modified plasmid was called pPS05 (Fig. 1) and was transformed via electroporation into *E. coli* DH5α first for analysis and amplification.

Plasmids were transformed into *P. putida* KT2440 using the protocol by Choi et al. (2006). Five milliliters of preculture of *P. putida* KT2440 were centrifuged in sterile 15 mL tubes for 3 min at 4180*g*. The pellet was resuspended in 2 mL of 300 mM cold sucrose solution and was centrifuged for 2 min at 17,000*g*. The pellet was then resuspended in 1 mL of 300 mM sucrose solution and centrifuged again. The pellet was once again resuspended in 100 µL of 300 mM sucrose and stored on ice. One to two microliters of plasmid preparation were mixed with 60 µL of the electrocompetent cells, filled in a cold sterile electroporation cuvette with an electrode gap of 2 mm and transferred to the Gene PulserXcell electroporator from BioRad (Hercules, CA, USA). The pulse was set to 2.500 V, 200 Ω and 5 ms.

T4 Ligase (Thermo Fisher Scientific, Waltham, MA, USA), the Gibson Assembly Cloning Kit (NEB, Ipswich, MA, USA), and restriction enzymes (Thermo Fisher Scientific, Waltham, MA, USA) were used routinely.

2.3. Analysis of rhamnolipids

The rhamnolipid concentration was determined by reversed-phase high-performance liquid chromatography (RP-HPLC). As an analytical column, a NUCLEODUR C18 Gravity (Macherey-Nagel GmbH & Co. KG, Düren, Germany) was used (dimensions: 150 × 4.6 mm; particle size: 3 µm). The HPLC system Ultimate 3000 was connected to a Corona-charged aerosol detector (CAD) (all Thermo Fisher Scientific Inc., Waltham, MA, USA). The flow rate was set to 1 mL/min, and the column oven temperature was maintained at 40 °C. Five microliters of the sample were injected. A binary gradient of acetonitrile and ultra-pure water supplied with 0.2% (*v*/*v*) formic acid was used. The acetonitrile concentration was increased linearly from 70% to 100% between 1 min and 9 min, and it was decreased linearly from 100% to 70% between 11 min and 12 min. One measurement was terminated after 15 min. The rhamnolipid concentration of *P. putida* cultures was measured after 3 days of cultivation. One milliliter of the suspension was centrifuged for 5 min at 17,000*g*. Five hundred microliters of the supernatant were subsequently mixed with 500 µL of acetonitrile and stored at 4 °C overnight. Subsequently, the sample was centrifuged for 5 min at 17,000*g*. One hundred fifty microliters of the supernatant were filtered using Phenex-RC syringe filters (diameter 4 mm, pore size 0.2 µm) (Phenomenex,

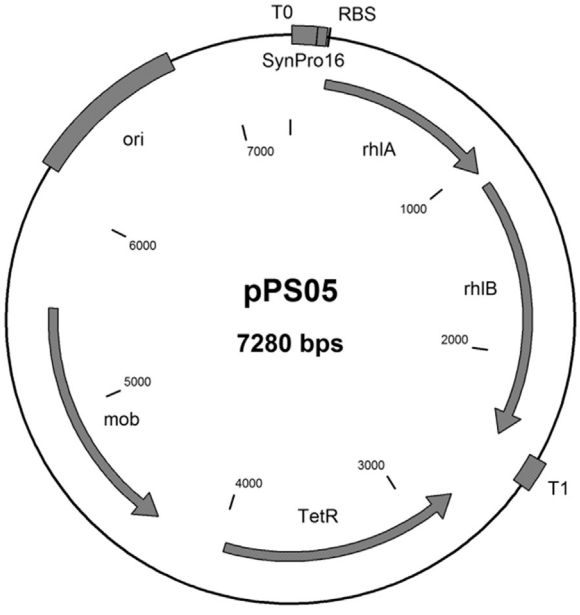

Fig. 1. Vector pPS05. Depicted are all of the important elements, including the genes *rhlA* and *rhlB*, the tetracycline resistance cassette (TetR), the terminators (T0 and T1), the origin of replication (ori), the promoter (SynPro), and the ribosomal binding site (RBS). The plasmid also carries a mobilization gene (mob).

Aschaffenburg, Germany) and pipetted into HPLC vials for subsequent HPLC analysis.

2.4. Flux estimation in supply pathways

The following assumptions were made to estimate the flux through the activated dTDP-rhamnose synthesis pathway. First, the content of lipopolysaccharides (LPS) per CDW in *P. putida* is similar to that in *P. aeruginosa*. Second, the number of rhamnose molecules incorporated into LPS is similar in both organisms. Darveau et al. determined the LPS of *P. aeruginosa* to account for 7.3% of the total CDW (Darveau and Hancock, 1983), whereas de Weger *et al*. reported that the LPS of *P. aeruginosa* consisted of 3.3% of rhamnose (de Weger et al., 1987). Hence, 0.24% of the CDW of *P. aeruginosa* and *P. putida* consists of rhamnose, amounting to 0.015 mmol rhamnose per g_{CDW}.

The flux through fatty acid *de novo* synthesis can be calculated accordingly. Approximately 10% of the CDW is composed of fatty acids (Stephanopoulos et al., 1998). A major constituent of the cell membrane in *P. putida* KT2440 is hexadecanoic acid (Rühl et al., 2012), with a molecular weight of 256 g/mol. *De novo* fatty acid synthesis hence requires $8C_2$ units, which results in 3.12 mmol fatty acid formed per g_{CDW}. Multiplied by the growth rate, the rate for fatty acid biosynthesis can be estimated.

2.5. Measurement of ^{13}C-labeled rhamnolipids

Sample preparation was performed according to Behrens et al. (2016). Rhamnolipid characterization was carried out on an Alliance 2695 separations module coupled to a micromass Quattro micro triple quadrupole mass spectrometer (both Waters Corporation, Milford, MA, USA). For separation, reversed-phase chromatography on a NUCLEODUR Sphinx RP (3 μm) was performed with a 2 mm × 150 mm column (Macherey-Nagel, Düren, Germany) at 40 °C with a flow rate of 0.3 mL/min. A binary gradient of acetonitrile (for HPLC, Gradient Grade; VWR International, Fontenay-sous-Bois, France) and 5 mM ammonium formate buffer (LC-MS Ultra, ≥ 99.0%; Sigma-Aldrich Chemie GmbH, Steinheim, Germany) at pH 3.3 were used as eluents. Mass spectrometric detection was performed by electrospray ionization in negative mode.

2.6. Measurement of carbon dioxide production

The produced carbon dioxide was measured using a BCP-CO_2 sensor with a PA-plastics housing and recorded using the software BacVis (all from BlueSens Gas Sensor GmbH, Herten, Germany). The sensor was screwed onto a special 1 L shake flask without baffles. The flask was filled with 100 mL of medium and shaken at 200 rpm with a throw of 50 mm at 30 °C.

3. Results and discussion

3.1. Synthetic promoter library

The expression vector used previously was pVLT31 (de Lorenzo et al., 1993) featuring the ori RSF1010 and the inducible *tac* promoter (de Boer et al., 1983). This vector was used here as a reference. The newly constructed plasmid is based on pBBR1-MSC3 (Kovach et al., 1995), containing the pBBR1 ori. The native RBS of the genes were kept. With *P. putida* carrying the synthesis pathway under the control of a synthetic promoter library indeed high rhamnolipid producing mutants were identified. From the first screening of a couple of thousand mutants using the blood agar assay, only 75 transformants were found to produce rhamnolipids (these results have partly been published in Beuker et al. (2016). 23 of these were characterized in more detail. Shake flask experiments were carried out with these strains to determine physiological data on rhamnolipid production. Surprisingly nine strains did not produce detectable amounts of rhamnolipids. The remaining 14 transformants covered a rhamnolipid titer range from 0.05 g/L to 2.8 g/L (Fig. 2). While the transformant with the reference expression system, featuring a *tac* promoter, only produced 0.31 g/L rhamnolipids (Wittgens et al., 2011), the best producing transformant carrying the variant no. eight of the synthetic promoter library produced up to 2.8 g/L and was called *P. putida* KT2440 pSynPro8. This microbial cell factory, with its constitutive expression system features simplified handling, as induction is no longer required.

Seven promoters were chosen for sequencing, covering the whole range of rhamnolipid titers. The data shows, that indeed the −35 and −10 box remained unchanged, while the randomized regions featured great variations in nucleotides. As all these promoters showed rhamnolipid production during the first screening, one might conclude that only intact promoters lead to the production of rhamnolipids.

```
SynPro8:   AGCTC TTGACA AGGTCGGAAAATTGAAG TATAAT
           ATCAGT
SynPro5:   TTTCC TTGACA AGCCTAGTTTCGCCATT TATAAT
           GACTCG
SynPro16:  GTTGA TTGACA AAGCGCTTACCTCTTTC TATAAT
           ATAGAG
SynPro1:   GGTGG TTGACA TTGGCATTACAACGTAT TATAAT
           TTAGCG
```

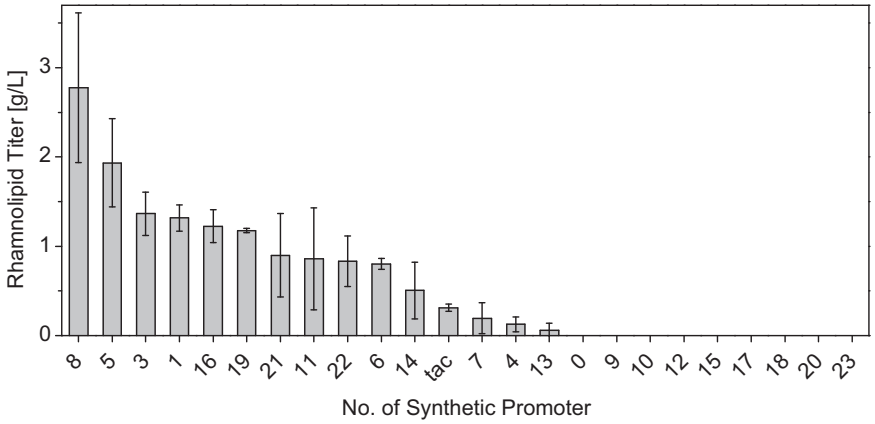

Fig. 2. Final rhamnolipid titers of *P. putida* with different synthetic promoters. The previously used *tac* promoter based system served as reference. The error bars represent the deviation from the mean of two biological replicates.

```
SynPro11:  TAGAG TTGACA CACCTTCGGGTGGGCCT TATAAT
           ACTCGC
SynPro7:   TATAT TTGACA GAACCCCTGCAGACGTA TATAAT
           ATGGTG
SynPro15:  TACGC TTGACA TCGTGCGCCGGGCTGGT TATAAT
           GCCGAA
```

3.2. Rhamnolipid-producing P. putida

With the best performing expression system pSynPro8, *P. putida* produced under reference conditions (10 g/L glucose in LB medium) approximately 3 g/L rhamnolipids (Fig. 3), corresponding to a carbon yield of 40% [$Cmol_{RL}/Cmol_{Glc}$], which is approximately 55% of the theoretical yield. Whereas the titers obtained with the native producer were higher with plant oils as carbon sources (> 100 g/L), the carbon yield of *P. aeruginosa* was 7% [$Cmol_{RL}/Cmol_{Glc}$], less than the 10% of the stoichiometric theoretical yield (Müller et al., 2010).

The titer achieved here was the highest reported using a recombinant rhamnolipid producer with glucose as a carbon source. Compared to our first strain *P. putida* KT42C1 pVLT31_*rhlAB* (Wittgens et al., 2011), a doubling in titers could be achieved (3 g/L instead of 1.5 g/L). As a result of the high titer and the short fermentation time, this new microbial cell factory featured a specific rhamnolipid production rate, which was approximately three times higher than it was with the first strain (47 mg/(g_{CDW} h) instead of 18 mg/(g_{CDW} h)). Strikingly, this rate was also approximately 75% higher than the rate that the wild-type producer features (27 mg/(g_{CDW} h)) (Table 3).

We would like to emphasize that the only alteration of the organism was the overexpression of the two dedicated genes *rhlA* and *rhlB*, resulting in the substantial production of a secondary metabolite in a host that generally produces biomass and CO_2.

Apparently, cell growth was limited after approximately 5 h. This behavior is often exhibited in cultivations with complex media, as shifting between carbon sources occurs. Once the preferred carbon source is depleted, the catabolism switches to the next carbon source, which is reflected in the growth curve. Consequences in the context of the described experiment could be reduced rhamnolipid production. On the contrary, an alternative effect could be enhanced rhamnolipid production, as limited growth frees more resources for rhamnolipid synthesis. Indeed an increase in the rhamnolipid production rate, indicated by a deviation of the experimental data above the fitted line can be inferred.

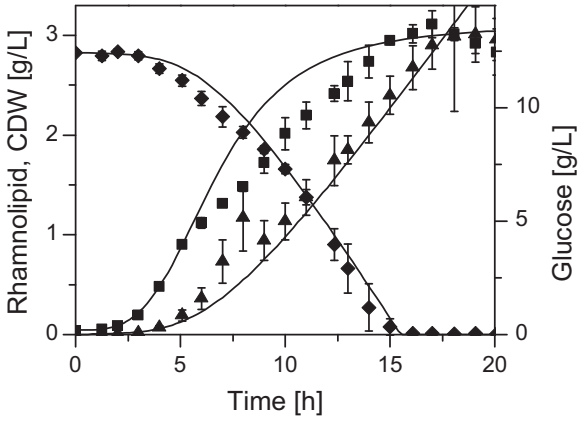

Fig. 3. Rhamnolipid production with *P. putida* KT2440 pSynPro8. Development of biomass (rectangles, ■), rhamnolipid (triangles, ▲), and glucose (diamonds, ◆) concentrations. The experimental data are depicted as symbols, and the lines present the fitted courses. The CDW trend was determined using a logistic growth model. A multivariable least squares fit was used to illustrate the development of all three fermentation parameters depending on each other, according to Wittgens et al. (2011). The error bars represent the deviation from the mean of two biological replicates. CDW, cell dry weight.

3.3. Meeting metabolic demands

We observed in the above experiments an increased glucose uptake rate of 1.2 mmol/(g_{CDW} h) for pPS05 and 3.2 mmol/(g_{CDW} h) for pSynPro8, which we here investigate conceptually. Can the metabolic network operation in *P. putida* be hijacked by creating demand for central carbon metabolism (CCM) intermediates? We previously showed that energetic demand could be met by *P. putida* by increasing the glucose uptake rate dramatically, for example, in response to a second phase of octanol (Blank et al., 2008) or the uncoupler 2,4-dinitrophenol (DNP) (Ebert et al., 2011).

To evaluate whether the metabolism of the *P. putida* used here, grown on a complex medium (e.g., amino acids available) and complemented with glucose, responds comparably, we added alternating DNP concentrations. When adding 700 mg/L DNP to *P. putida* KT2440 growing in LB medium supplemented with 10 g/L glucose, the strain had a glucose uptake rate of 2.0 mmol/(g_{CDW} h) instead of 1.1 mmol/(g_{CDW} h) without DNP. At a concentration of 1,100 mg/L DNP, the glucose uptake rate reached 2.2 mmol/(g_{CDW} h). This increase in glucose uptake rate did not affect the growth rates, which were 0.86 h^{-1} (no DNP), 0.88 h^{-1} (700 mg/L DNP), and 0.79 h^{-1} (1,100 mg/L DNP) (Fig. 4). Importantly, no byproduct formation was observed, consistent with Blank et al. (2008) and Ebert Ebert et al. (2011). Hence, creating a sink for NADH by the addition of an uncoupler resulted in a doubling of the glucose uptake rate. This finding provides strong support that the metabolic network operation of *P. putida* can be substantially altered by the here-exploited concept of driven by demand.

3.4. Hijacking central carbon metabolism operation

Can the observed increase in glucose uptake rate be exploited for the production of valuable chemicals? We previously reported that the CCM in *P. putida* is, under many conditions, not regulated transcriptionally but, rather, at the metabolic (and potentially posttranslational) level. In contrast, peripheral anabolic and catabolic pathways are transcriptionally regulated (Sudarsan et al., 2014). This organization of the metabolic network allows for rapid flux rerouting to adapt to ever-changing growth conditions. We here argue again that these flux changes are the result of changing metabolic demands (Table 2).

Consequently, we examined whether this structural

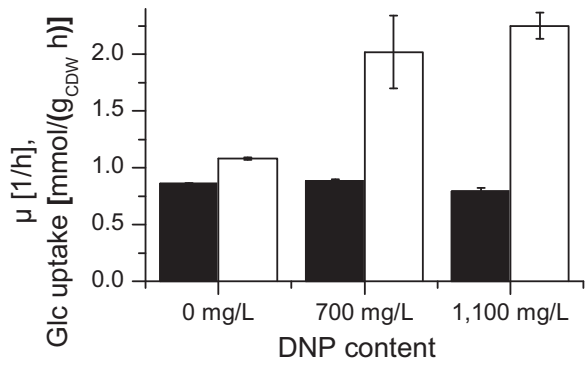

Fig. 4. 2,4-Dinitrophenol (DNP) addition leads to enhanced glucose uptake rates. The specific glucose uptake rate is shown in white, and the growth rate is depicted by the black-filled columns. *P. putida* KT2440 pPS05 was cultivated without DNP as a reference and with 700 and 1,100 mg/L DNP, according to Ebert et al. (2011). The error bars represent the deviation from the mean of two biological replicates.

Table 2
Changing flux through CCM during growth ($\mu = 0.1$ 1/h) on different carbon sources in *P. putida* KT2440 (Sudarsan et al., 2014). PP – pentose phosphate, TCA – tricarboxylic acid.

Substrate	Flux through pathway [mmol/(g_{CDW} h)]		
	PP pathway	Lower glycolysis	TCA cycle
Glucose	0.01	2.13	2.98
Fructose	0.03	1.53	1.87
Benzoate	0.00	0.18	0.57

organization of the metabolic network explained the high performance of the rhamnolipid-synthesizing strain (Fig. 3). We introduced the genes for mono-rhamnolipid synthesis into *P. putida* (*rhlA* and *rhlB*), thereby creating additional demand in the CCM for glucose-6-phosphate (for rhamnose synthesis) and acetyl-CoA (for hydroxy-fatty acid production via *de novo* lipid synthesis) (Fig. 5).

To examine different demands, i.e., different rhamnolipid production rates, we used the two plasmids pSynPro8 and pPS05 and two strains, namely, the reference *P. putida* KT2440 and the derivative *P. putida* KT40CZC. In *P. putida* KT40CZC, the PHA synthesis operon is deleted (Escapa et al., 2012). PHA synthesis starts from activated hydroxy-fatty acids competing directly with rhamnolipid synthesis for the common precursor. Quantitative physiology experiments allowed for the estimation of flux via the precursor-supplying pathways, the glucose uptake rate, and the growth rate. For comparison, the physiology of the reference strain *P. putida* KT2440 not producing rhamnolipids was examined.

It was discovered that *P. putida* KT40CZC was better suited for rhamnolipid synthesis with the new expression plasmid pPS05 than the wild-type strain (Table 3). This recombinant strain has a higher specific production rate and also reaches a higher titer.

With an increasing rhamnolipid production rate, the glucose uptake increased while the growth rate remained constant (Fig. 6). In the best producing strain with a rhamnolipid production rate of 0.1 mmol/(g_{CDW} h), the glucose uptake increased by 24% to 1.3 mmol/(g_{CDW} h) compared to the non-producing strain. *P. putida* KT2440 pPS05 produced rhamnolipids with a glucose uptake rate of 1.2 mmol/(g_{CDW} h), which is 12% more than the wild-type strain. These findings are a strong indication that flux through the CCM is indeed increased. The additional glucose is used to satisfy the increased demand created by the production of the rhamnolipids.

To assess whether the extra glucose, which is taken up is directed to rhamnolipid synthesis or just burned and oxidized to carbon dioxide, CO_2 production was measured in a separate experiment. As can be seen, carbon dioxide production of the reference *P. putida* KT2440 is higher compared to the rhamnolipid producer (Fig. 7). The reduction in CO_2 formation might be a response of *P. putida* to the availability of an additional redox sink, namely rhamnolipid synthesis. The reference strain oxidizes glucose to CO_2 via the tricarboxylic acid (TCA) cycle. To regenerate the reduced redox cofactors and thereby balance the electrons, the electron transport chain is employed by *P. putida* using oxygen as terminal electron acceptor. The rhamnolipid-producing strain can use the rhamnolipids as electron acceptors as the carbons in the fatty acid moieties are higher reduced than glucose. Thus, we assume that this strain under the given conditions does not need the electron transport chain to the same extend as the reference strain, with the result of lower CO_2 formation.

As less glucose is wasted for the generation of CO_2, the rhamnolipid production strain should be able to allocate more carbon to the synthesis of rhamnolipids. These considerations again hint to the conclusion that via reorganization of metabolic fluxes the cell is able to meet the opposed demand.

Based on the physiological data, we estimated the flux through

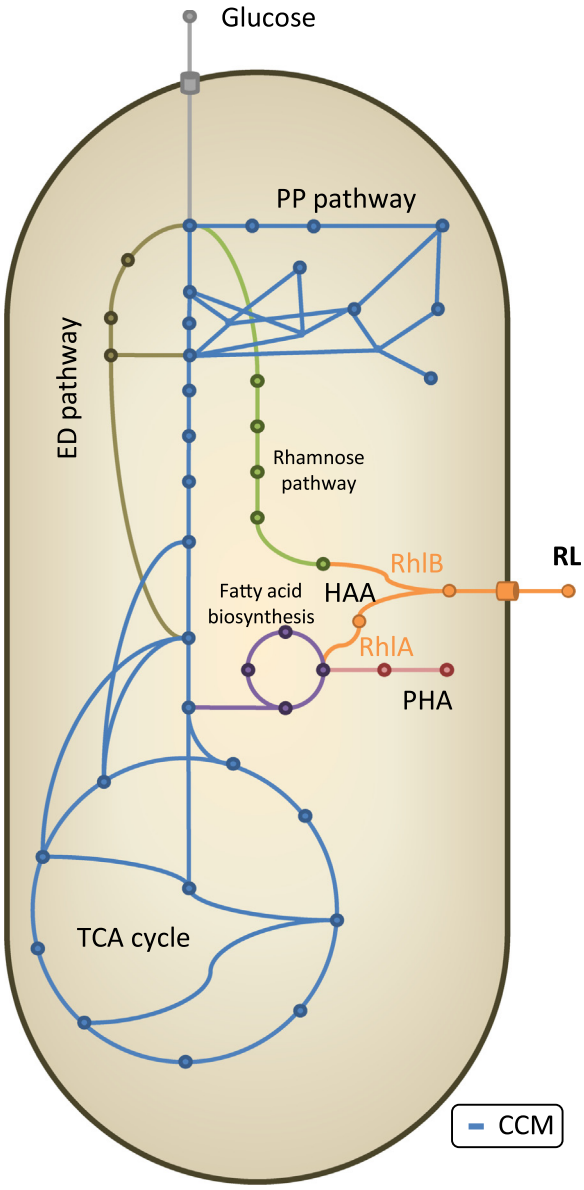

Fig. 5. Rhamnolipid biosynthesis pathway. The blue lines depict the CCM after Sudarsan et al. (2014), including the pentose phosphate (PP) pathway and tricarboxylic acid (TCA) cycle, and the brown lines represent the Entner-Doudoroff (ED) pathway. The green and the purple lines indicate the rhamnolipid precursor-providing pathways: the rhamnose pathway, and fatty acid biosynthesis, respectively. The red lines show the competing polyhydroxyalkanoate (PHA) production, and the orange lines symbolize the introduced rhamnolipid (RL) synthesis pathway. The recombinant enzymes (RhlA and RhlB) originating from *P. aeruginosa* and introduced in *P. putida* by the encoding genes are indicated in orange. These were the only genetic modifications implemented. (For interpretation of the references to color in this figure legend, the reader is referred to the web version of this article.)

the pathways providing the precursors for rhamnolipid production, i.e., activated dTDP-rhamnose, and the hydroxy-fatty acids for HAA synthesis (Fig. 8). The *P. putida* wild type not producing rhamnolipids still synthesizes rhamnose as part of the lipopolysaccharides on the outer cell wall. A constant synthesis rate was estimated based on the growth rate and on the approximate rhamnose content in the lipopolysaccharides. For *de novo* synthesis, basic activity was calculated via the fatty acid share in the biomass. When introducing the enzymes for rhamnolipid production, the particular flux via the activated rhamnose pathway was dramatically enhanced. Moreover, *de novo* fatty acid synthesis increased by 50% in the best producing strain.

Again, these enhancements of flux in the metabolic network

Table 3
Growth and production parameters of rhamnolipid synthesis. For comparison, wild-type *P. aeruginosa* PA01 is listed in line 1.

Organism	Medium	Substrates		Cell Dry Weight	Maximal Titer	Carbon Yield[a]	Process Time	Space-Time Yield	Specific RL-Prod. Rate[b]	Reference
		Substance	[g/L]	[g_{CDW}/L]	[g_{RL}/L]	[$Cmol_{RL}$/$Cmol_{subs}$]	[h]	[mg_{RL}/(L h)]	[$g/(g_{CDW}$ h)]	
P. aeruginosa PA01	MS	Sunflower Oil	250	16.3	39.0	0.07 (8%)	90	433.3	0.027	Müller et al. (2010)
P. putida KT2440 pSynPro8	LB	Glucose	12	3.1	3.2	0.40 (55%)	22	146.4	0.047	Wittgens (2013)
P. putida KT40CZC pPS05	LB	Glucose	11	3.4	2.4	0.35 (48%)	23	104.3	0.031	This study
P. putida KT2440 pPS05	LB	Glucose	11	4.5	2.2	0.32 (44%)	22	100.0	0.022	This study

LB – Lysogeny broth, MS – Mineral salts.

[a] For the calculation of yields during production on complex media, it was assumed that rhamnolipids were synthesized from glucose, whereas other medium components were utilized for cell growth. The numbers in parentheses show the percentages of the theoretical maximum.

[b] The specific rhamnolipid production rate was calculated as the average over the entire fermentation time using the maximal rhamnolipid titer and the maximal cell dry weight determined.

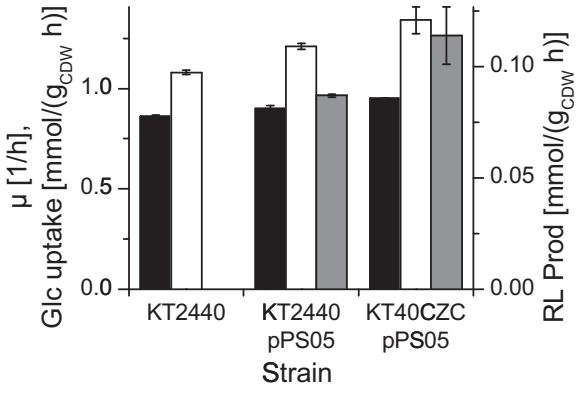

Fig. 6. Performance parameters of rhamnolipid producers compared to the wild-type strain. The black-filled columns represent the growth rate, and the unfilled columns indicate the glucose uptake rate. On the second y-axis, specific rhamnolipid production is plotted. The respective columns are filled in gray. For better comprehension, the second y-axis is also drawn in gray. The error bars represent the deviation from the mean of two biological replicates.

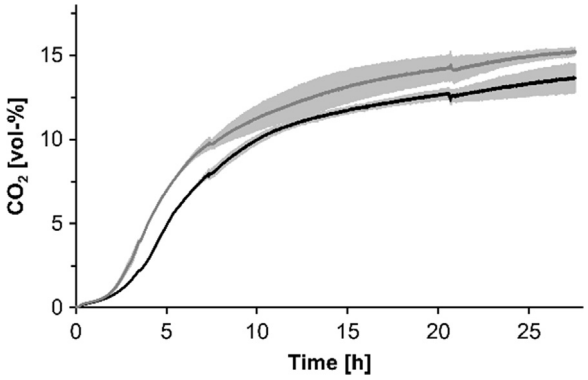

Fig. 7. Carbon dioxide produced during cultivation by *P. putida* KT2440 (gray line) and *P. putida* KT2440 pPS05, which is capable of rhamnolipid synthesis (black line). The deviation shown in light gray originates from the mean of two biological replicates.

occurred without any engineering of the CCM. Rather, the metabolism met the demand created, which was possible because *P. putida* is capable of up-regulating its CCM on a metabolic level without altering gene expression levels (Sudarsan et al., 2014). Because rhamnose is synthesized from glucose-6-phosphate and fatty acid *de novo* synthesis also draws carbon from CCM, and furthermore, growth remains constant, the flux distribution in the

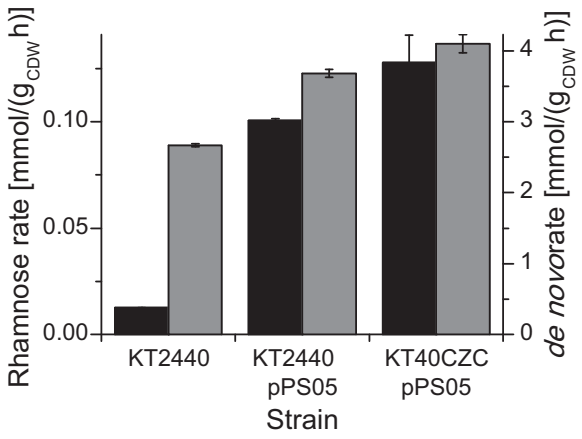

Fig. 8. Estimated intracellular fluxes in *P. putida* strains with different activity levels of rhamnolipid production. The black-filled columns represent the rate via the rhamnose pathway, and the gray-filled columns indicate the *de novo* fatty acid synthesis rate (second y-axis). For better comprehension, the second y-axis is also shown in gray. The error bars represent the deviation from the mean of two biological replicates.

CCM is clearly altered to meet the RL synthesis demand.

Metabolic engineering strategies often involve the increase of flux in precursor-providing pathways. To identify valuable targets for overexpression, metabolic control analysis is frequently performed. Metabolic control analysis examines the underlying reaction network of a given pathway to distinguish the enzymatic step that controls the overall production rate. This specific reaction rate can then be enhanced, which should lead to a higher production rate toward the product of choice. This process is continued iteratively until no further enhancement can be achieved (Stephanopoulos et al., 1998).

To increase rhamnolipid production, it would thus be advisable to overexpress the entire *rml* operon harboring the genes responsible for the synthesis of the activated dTDP-rhamnose from glucose-1-phosphate or the pyruvate dehydrogenase, which is the first step from pyruvate toward *de novo* lipid synthesis (Scriba and Holzer, 1961). A substantial enhancement of flux in glucose-6-phosphate- and pyruvate-supplying pathways via CCM is required to sustain an unchanged rate of growth and to generate the resources for the heterologous production of rhamnolipids (Fig. 5).

We hence conclude that CCM operation in *P. putida* is driven by the demand created. Again, the mechanistic explanation might be that the CCM in this organism is regulated at the metabolic level (Sudarsan et al., 2014). Hence, generating additional demand by

introducing enzymes deriving metabolites from CCM causes *P. putida* to increase metabolic flux. In the presented example, we overexpressed two enzymes producing rhamnolipids, which burdened CCM at glucose-6-phosphate and acetyl-CoA, resulting in flux increases by 300% and 50%, respectively.

There is however one major difference to the experiment carried out by Sudarsan et al., (2014). While they were working in a chemostat environment at constant growth rate, the experiments described here were carried out in batch cultures, featuring different growth phases. In the previous study, the putative impact of growth rate on transcriptional regulation was thus excluded by the experimental setup, while this has not been done in the experiments carried out in this study. Differences in growth could thus be partly responsible for the observed phenomena.

The conditions under which an organism responds to being driven by demand is not generally known. *Pseudomonas,* as a soil bacterium, lives in environments where nutrients are scarce and must compete for these resources. Other industrial microorganisms, such as *E. coli*, *Lactobacillus*, and *Saccharomyces cerevisiae,* have been isolated from nutrient-rich environments, such as the lower intestines of mammals, milk, and crops, respectively. With many resources in abundance, these organisms might have been selected for rate rather than for efficiency (yield) (Novak et al., 2006; Jessup and Bohannan, 2008).

A good example for the high efficiency of *P. putida* is its glucose uptake system. Whereas *E. coli* and other microorganisms absorb glucose at high rate, *P. putida* converts part of the glucose into gluconate and further into ketogluconate (del Castillo et al., 2007). This process has two advantages in a competitive environment. First, while growing on a preferred carbon source, the bacterium renders this carbon source useless for competitors not able to absorb gluconate or ketogluconate. Second, gluconate and ketogluconate are organic acids and thus greatly lower the pH. A low pH not only stops the growth of some organisms but also frees some of the scarce resources, such as iron and phosphate (Rodriguez and Fraga, 1999).

Another interesting feature of the glucose uptake system of *P. putida* is its superior glucose affinity. Glucose uptake in *P. putida* into the periplasmic space occurs through outer membrane porins encoded by *oprB1* and *oprB2*. The importation into the cytosol is mediated through an ABC uptake system encoded by the open reading frames PP1015 to PP1018 (del Castillo et al., 2007). ABC transporters in Gram-negative bacteria often feature a binding protein that is located in the periplasm. This binding protein has high affinity for the specific substrate (Boos et al., 1996). The transport system of *Thermococcus litoralis,* featuring a similar binding protein, for example, has a K_m of approximately 20 nM, whereas the K_m of the glucose uptake system of *E. coli* exhibits 1 μM (Xavier et al., 1996). After binding the substrate, the actual transport is driven by the hydrolysis of ATP molecules (Davidson and Chen, 2004). This biochemical investment allows for glucose uptake when concentrations are very low.

These two examples show the adaptation of *P. putida* to environments where nutrients are scarce. Under such conditions, changes in carbon sources are frequent. Whenever a change in the environment occurs, *P. putida* is able to reconfigure its CCM rapidly without relying on transcriptional regulation. In the context of heterologous rhamnolipid production, which is an engineered demand, *P. putida* increases carbon uptake while maintaining a high growth rate. The metabolism simply reacts to the “theft” of precursors needed for growth by increasing the flux through the essential precursor pathways.

3.5. Glucose satisfies the enhanced carbon demand

As described above, the rate of glucose uptake increases when an additional demand is created. Is this glucose directed toward rhamnolipid synthesis and hence to the created demand, or is it simply distributed throughout the bacterium's metabolism? Via stable isotope-labeling experiments and the analysis of the resulting labeling patterns in the rhamnolipid molecules, the carbon source used for rhamnolipid synthesis was determined.

For the corresponding experiments, on the one hand, minimal medium supplemented with unlabeled glucose and, on the other hand, LB medium with uniformly ^{13}C-labeled glucose were used. Two samples were obtained: one in the exponential phase and the other in the stationary phase. At the latter time point, the glucose was completely consumed. The synthesized rhamnolipids were analyzed by HPLC coupled to mass spectrometric detection (LC–MS). The produced biomass was investigated by gas chromatography coupled to mass spectrometry (GC–MS) measurement. Sections of the LC-MS mass spectra at the retention time of Rha-C_{10}-C_{10} (11.8 min) are depicted in Fig. 9.

The molecular weight of the Rha-C_{10}-C_{10} rhamnolipid molecule is 504 u. It is detected as a deprotonated molecule (mass to charge ratio [*m/z*] of 503) during LC-MS analysis with electrospray ionization. In the mass spectra shown in Fig. 9, the measured signals are higher than *m/z* 503 caused by ^{13}C-incorporation from the labeled glucose precursor. The examined rhamnolipid Rha-C_{10}-C_{10} contains 26 carbon atoms; thus, signals from *m/z* 503 to *m/z* 529 can occur. A fully labeled rhamnolipid would give rise to *m/z* 529.

Mass spectra a and d show the rhamnolipid Rha-C_{10}-C_{10} synthesized from unlabeled glucose in different growth phases as a reference. The highest peak is at *m/z* 503. Mass spectrum b, obtained from cultivation in minimal medium with fully labeled glucose, should show only the *m/z* 529 signal. However, as shown in Fig. 9b, the measured rhamnolipids show a distribution with its maximum at *m/z* 517. The explanation for this distribution in partially labeled rhamnolipid is the presence of unlabeled biomass from the preculture and the percentage of unlabeled glucose, which is contained in the ^{13}C-labeled glucose. The enrichment of ^{13}C-labeled glucose is 99% for each carbon atom, resulting in 94% (0.99^6) completely labeled glucose molecules. Interestingly, the mass spectra for the rhamnolipid derived from the cultivation with ^{13}C-labeled glucose with minimal medium (Fig. 9b) and LB medium (Fig. 9c) are very similar, indicating that during the exponential phase, the main source for rhamnolipid production is glucose, whereas the components of the LB medium are consumed for cell growth. Spectrum e shows the expected distribution: almost exclusively fully labeled rhamnolipid Rha-C_{10}-C_{10}. The distribution in spectrum f is also shifted toward higher masses, again showing that the main carbon source for rhamnolipid synthesis is glucose. During the exponential phase (Fig. 9c), this leads to a spectrum similar to the spectrum of the rhamnolipid when using isotopically labeled glucose as sole carbon source (Fig. 9b). Later, when the unlabeled compounds are further attenuated by the depletion of media components and the comparatively higher influx of labeled carbon atoms, the labeling pattern of the rhamnolipid shifts to higher masses (Fig. 9f).

An interesting observation is that, in the mass spectra, the *m/z* values with even numbers also appear, despite *de novo* fatty acid synthesis assembling fatty acids using C_2 molecules as basic modules. In theory, the labeling of the rhamnolipid molecules should thus increase in steps of two. The unlabeled carbon that is incorporated into the rhamnolipid molecule, however, also contains natural ^{13}C-isotopes. The natural abundance of ^{13}C is 1.08. In the rhamnolipid molecule, which contains 26 carbon atoms, this results in almost 29% of the molecules having one ^{13}C-isotope and approximately 4% of the total rhamnolipid molecules carrying two ^{13}C-isotopes. Furthermore, isotope ratios of O (^{16}O=100%; ^{17}O=0.04%; ^{18}O=0.21%;) and H (^{1}H=100%; ^{2}H=0.01%) contribute to the signals. This naturally occurring isotope distribution is

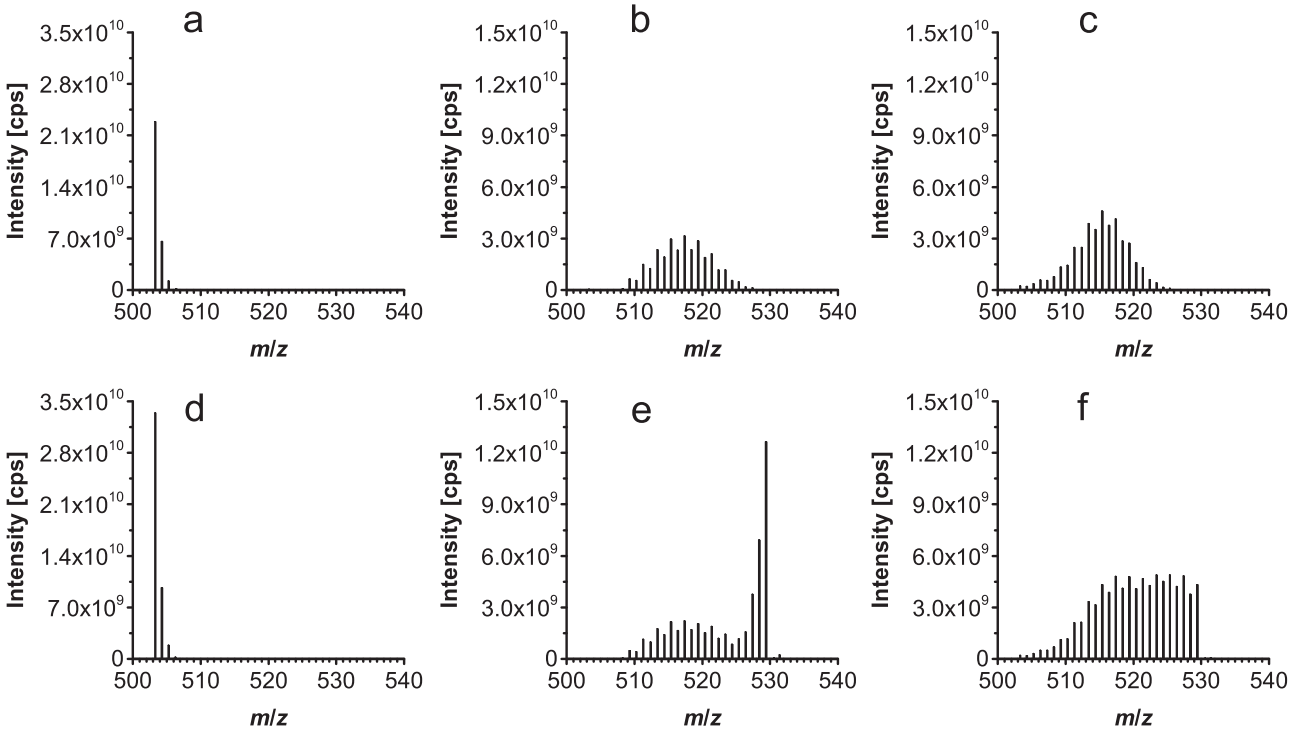

Fig. 9. Mass spectra of LC–MS measurements of the rhamnolipid Rha-C_{10}-C_{10}. The mass spectra show data for the rhamnolipid Rha-C_{10}-C_{10} synthesized by *P. putida* KT2440 pPS05 grown in LB or minimal medium with unlabeled or ^{13}C-labeled glucose in two distinct growth phases: a) minimal medium and ^{12}C-glucose, exponential phase; b) minimal medium and ^{13}C-glucose, exponential phase; c) LB medium and ^{13}C-glucose, exponential phase; d) minimal medium and ^{12}C-glucose, stationary phase; e) minimal medium and ^{13}C-glucose; stationary phase; and f) LB medium and ^{13}C-glucose, stationary phase. Isotope distribution in a) and d) reflects the natural abundance of ^{13}C (1.1%), which corresponds to approximately 29% for 26 carbon atoms of *m*/*z* 504. cps – counts per second.

reflected in mass spectra a and d.

We also performed the reverse test, measuring the labeling in the proteinogenic amino acids. The fractional labeling of the examined amino acids showed that most amino acids were absorbed from the medium, whereas only a minor fraction was synthesized *de novo* from glucose (Fig. 10). Whereas some amino acids showed a fractional labeling of more than 0.2, at least half of the analyzed amino acids featured a fractional labeling less than 0.1; hence, more than 90% of these amino acids were absorbed from the medium.

To conclude, we showed that the synthesized rhamnolipids mainly originated from the ^{13}C-labeled glucose, whereas the biomass predominantly originated from unlabeled medium compounds. Hence, the increased glucose uptake caused by the created demand was most likely used by the cell to satisfy this demand. The sugars were directed by the metabolism of *P. putida* toward the reactions providing precursors for rhamnolipid synthesis. Only a minor fraction of the sugar was used for biomass production. In addition, the carbon dioxide production experiments point to the conclusion that rhamnolipid synthesis offers a possibility for the cell to use the offered carbon source more efficiently. Thus, the production strain is able to invest more glucose for the synthesis of rhamnolipids.

The yield of product on substrate is an important parameter in biocatalysis. One challenge is the reduction of yield caused by the growth of the whole-cell catalyst. Hence, production under reduced- or non-growth conditions is an engineering goal. We reported previously that engineered *P. putida* KT2440, under reference conditions, produced rhamnolipids independently of growth (Wittgens et al., 2011). The carbon source used (LB or glucose) was inferred from CO_2 evolution. Here, we report the direct measurements of the ^{12}C/^{13}C-labeling of rhamnolipids and the produced biomass.

The detected labeling patterns supported the hypothesis that

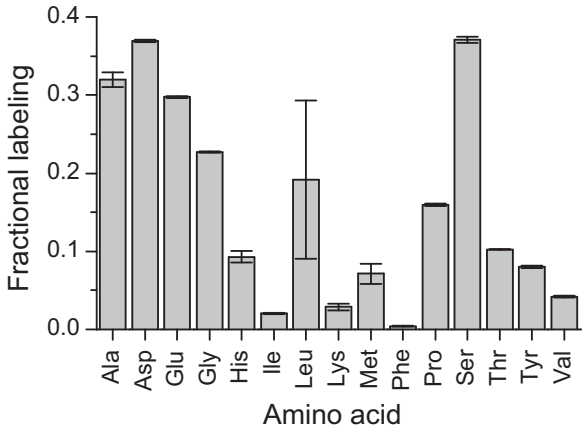

Fig. 10. Fractional labeling of amino acids during growth on LB medium with ^{13}C-labeled glucose. The fractional labeling indicates the fraction of carbon atoms in the respective molecule that are ^{13}C-labeled. The error bars represent the deviation from the mean of two biological replicates.

rhamnolipid synthesis occurred independently of growth. When supplying LB medium and ^{13}C-labeled glucose, the majority of the rhamnolipid molecules contained labeled ^{13}C-carbon atoms emanating from the labeled glucose. The fractional labeling in the exponential growth phase of the C_{10}-C_{10} rhamnolipids was 0.63. Only a small part (approximately 15%) of the rhamnolipid molecules carried ten or fewer labeled carbon atoms. Hence, the compounds from the LB medium contributed only a small fraction to rhamnolipid synthesis. In contrast, only 16% of the carbon atoms in the biogenic amino acids were labeled. The majority of the biomass is thus derived from unlabeled compounds of the medium and not from glucose. The assumption that medium compounds are used for growth while glucose is utilized in rhamnolipid

synthesis is thus strengthened.

A possible explanation for the uncoupling of growth and rhamnolipid production might be found in the lipidic precursor, i.e., the activated hydroxy-fatty acids. These molecules are also used for the synthesis of the internal storage polymer PHA, which *P. putida* produces during secondary substrate-limiting conditions when the carbon source is still abundant (Prieto et al., 2007).

4. Conclusion

In this work, we showed that the concept of "driven by demand" described for *E. coli* by Koebmann et al. (2002) could also be exploited for flux rerouting in *P. putida*. To rapidly implement heterologous pathways, tools for creating the required demand are becoming important (Zobel et al., 2015; Nikel et al., 2014). Interestingly, in the engineered microorganism, the production of the product of choice is uncoupled from growth, which might be caused by overcoming the host's intrinsic regulation cascades by introducing the target genes under the control of a synthetic promoter.

The results suggest that *P. putida* is a suitable host for biotechnological applications. Its versatile metabolism, which responds to the demand created by heterologous pathways, is well suited for metabolic engineering. Metabolic engineering of bacteria yielding a production strain, which is competitive on an industrial scale, is a complex task. Even for scientific groups with both the equipment and the required expertise, this process requires considerable time and effort, as demonstrated by the excellent extant examples (Becker et al., 2011; Becker and Wittmann, 2012a, 2012b; Buschke et al., 2013). *P. putida* might provide a good starting point for establishing novel synthesis pathways via classic metabolic engineering strategies.

Acknowledgements

The authors are grateful to Sandra Bennink (RWTH Aachen University) for her experimental help and to Susanne Wilhelm (Heinrich-Heine-University Düsseldorf) for helpful and inspiring discussions. The Deutsche Bundesstiftung Umwelt (DBU) (AZ13235) is gratefully acknowledged for providing financial support. This work was also partially funded by the Cluster of Excellence "Tailor-Made Fuels from Biomass," which is funded by the Excellence Initiative of the German federal and state governments to promote science and research at German universities.

References

Becker, J., Wittmann, C., 2012a. Systems and synthetic metabolic engineering for amino acid production – the heartbeat of industrial strain development. Curr. Opin. Biotechnol. 23 (5), 718–726.

Becker, J., Wittmann, C., 2012b. Bio-based production of chemicals, materials and fuels – *Corynebacterium glutamicum* as versatile cell factory. Curr. Opin. Biotechnol. 23 (4), 631–640.

Becker, J., Zelder, O., Hafner, S., Schroder, H., Wittmann, C., 2011. From zero to hero – design-based systems metabolic engineering of *Corynebacterium glutamicum* for L-lysine production. Metab. Eng. 13 (2), 159–168.

Behrens, B., Engelen, J., Tiso, T., Blank, L.M., Hayen, H., 2016. Characterization of rhamnolipids by liquid chromatography/mass spectrometry after solid-phase extraction. Anal. Bioanal. Chem. 408 (10), 2505–2514.

Bertani, G., 1951. Studies on lysogenesis I.: the mode of phage liberation by lysogenic *Escherichia coli*. J. Bacteriol. 62 (3), 293–300.

Beuker, J., Steier, A., Wittgens, A., Rosenau, F., Henkel, M., Hausmann, R., 2016. Integrated foam fractionation for heterologous rhamnolipid production with recombinant Pseudomonas putida in a bioreactor. AMB Express 6 (1), 11.

Blank, L.M., Ionidis, G., Ebert, B.E., Bühler, B., Schmid, A., 2008. Metabolic response of Pseudomonas putida during redox biocatalysis in the presence of a second octanol phase. FEBS J. 275 (20), 5173–5190.

de Boer, H.A., Comstock, L.J., Vasser, M., 1983. The tac promoter – a functional hybrid derived from the trp and lac promoters. Proc. Natl. Acad. Sci. – Biol. 80 (1), 21–25.

Boos, W., Lucht, J., 1996. Periplasmic binding protein-dependent ABC transporters. In: Neidhardt, F., et al. (Eds.), Escherichia coli and Salmonella typhimurium: Cellular and Molecular Biology. ASM Press, Washington, DC, pp. 1175–1209.

Buschke, N., Schafer, R., Becker, J., Wittmann, C., 2013. Metabolic engineering of industrial platform microorganisms for biorefinery applications – optimization of substrate spectrum and process robustness by rational and evolutive strategies. Bioresour. Technol. 135, 544–554.

del Castillo, T., Ramos, J.L., Rodriguez-Herva, J.J., Fuhrer, T., Sauer, U., Duque, E., 2007. Convergent peripheral pathways catalyze initial glucose catabolism in Pseudomonas putida: genomic and flux analysis. J. Bacteriol. 189 (14), 5142–5152.

Choi, K.H., Kumar, A., Schweizer, H.P., 2006. A 10-min method for preparation of highly electrocompetent Pseudomonas aeruginosa cells: application for DNA fragment transfer between chromosomes and plasmid transformation. J. Microbiol. Methods 64 (3), 391–397.

Darveau, R.P., Hancock, R.E.W., 1983. Procedure for isolation of bacterial lipopolysaccharides from both smooth and rough *Pseudomonas aeruginosa* and Salmonella typhimurium strains. J. Bacteriol. 155 (2), 831–838.

Davidson, A.L., Chen, J., 2004. ATP-binding cassette transporters in bacteria. Annu. Rev. Biochem. 73, 241–268.

Ebert, B.E., Kurth, F., Grund, M., Blank, L.M., Schmid, A., 2011. Response of Pseudomonas putida KT2440 to increased NADH and ATP demand. Appl. Environ. Microbiol. 77 (18), 6597–6605.

Escapa, I.F., Del Cerro, C., Garcia, J.L., Prieto, M.A., 2012. The role of GlpR repressor in Pseudomonas putida KT2440 growth and PHA production from glycerol. Environ. Microbiol. 15 (1), 93–110.

Hanahan, D., 1983. Studies on transformation of *Escherichia coli* with plasmids. J. Mol. Biol. 166 (4), 557–580.

Jensen, P.R., Hammer, K., 1998. The sequence of spacers between the consensus sequences modulates the strength of prokaryotic promoters. Appl. Environ. Micro. 61 (1), 82–87.

Jessup, C.M., Bohannan, B.J.M., 2008. The shape of an ecological trade-off varies with environment. Ecol. Lett. 11 (9), 947–959.

Koebmann, B.J., Westerhoff, H.V., Snoep, J.L., Nilsson, D., Jensen, P.R., 2002. The glycolytic flux in Escherichia coli is controlled by the demand for ATP. J. Bacteriol. 184 (14), 3909–3916.

Kovach, M.E., Elzer, P.H., Hill, D.S., Robertson, G.T., Farris, M.A., Roop II, R.M., Peterson, K.M., 1995. Four new derivatives of the broad-host-range cloning vector pBBR1MCS, carrying different antibiotic-resistance cassettes. Gene 166 (1), 175–176.

de Lorenzo, V., Eltis, L., Kessler, B., Timmis, K.N., 1993. Analysis of Pseudomonas gene products using $lacI^q$/Ptrp-lac plasmids and transposons that confer conditional phenotypes. Gene 123 (1), 17–24.

Müller, M.M., Hörmann, B., Syldatk, C., Hausmann, R., 2010. Pseudomonas aeruginosa PAO1 as a model for rhamnolipid production in bioreactor systems. Appl. Microbiol. Biotechnol. 87 (1), 167–174.

Nelson, K.E., Weinel, C., Paulsen, I.T., Dodson, R.J., Hilbert, H., Martins dos Santos, V. A.P., Fouts, D.E., Gill, S.R., Pop, M., Holmes, M., Brinkac, L., Beanan, M., DeBoy, R. T., Daugherty, S., Kolonay, J., Madupu, R., Nelson, W., White, O., Peterson, J., Khouri, H., Hance, I., Lee, P.C., Holtzapple, E., Scanlan, D., Tran, K., Moazzez, A., Utterback, T., Rizzo, M., Lee, K., Kosack, D., Moestl, D., Wedler, H., Lauber, J., Stjepandic, D., Hoheisel, J., Straetz, M., Heim, S., Kiewitz, C., Eisen, J., Timmis, K. N., Düsterhöft, A., Tümmler, B., Fraser, C.M., 2002. Complete genome sequence and comparative analysis of the metabolically versatile Pseudomonas putida KT2440. Environ. Micro. 4 (12), 799–808.

Nikel, P.I., Martinez-Garcia, E., de Lorenzo, V., 2014. Biotechnological domestication of pseudomonads using synthetic biology. Nat. Rev. *Microbiol.* 12 (5), 368–379.

Noor, E., Eden, E., Milo, R., Alon, U., 2010. Central carbon metabolism as a minimal biochemical walk between precursors for biomass and energy. Mol. Cell 39 (5), 809–820.

Novak, M., Pfeiffer, T., Lenski, R.E., Sauer, U., Bonhoeffer, S., 2006. Experimental tests for an evolutionary trade-off between growth rate and yield in *E. coli*. Am. Nat. 168 (2), 242–251.

Ochsner, U.A., Fiechter, A., Reiser, J., 1994. Isolation, characterization, and expression in Escherichia coli of the Pseudomonas aeruginosa rhlAB genes encoding a rhamnosyltransferase involved in rhamnolipid biosurfactant synthesis. J. Biol. Chem. 269 (31), 19787–19795.

Poblete-Castro, I., Binger, D., Rodrigues, A., Becker, J., Dos Santos, V.A. Martins, Wittmann, C., 2013. In-silico-driven metabolic engineering of Pseudomonas putida for enhanced production of poly-hydroxyalkanoates. Metab. Eng. 15, 113–123.

Prieto, M.A., de Eugenio, L.I., Galán, B., Luengo, J.M., Witholt, B., 2007. Synthesis and degradation of polyhydroxyalkanoates. In: Ramos, J.-L., Filloux, A. (Eds.), Pseudomonas. Springer, Netherlands, pp. 397–428.

Ramos, J.L., Duque, E., Huertas, M.-J., Haidour, A., 1995. Isolation and expansion of the catabolic potential of a Pseudomonas putida strain able to grow in the presence of high concentrations of aromatic hydrocarbons. J. Bacteriol. 177 (14), 3911–3916.

Rodriguez, H., Fraga, R., 1999. Phosphate solubilizing bacteria and their role in plant growth promotion. Biotechnol. Adv. 17 (4–5), 319–339.

Rühl, J., 2012. Characterization and Engineering of Pseudomonas Putida for Aerobic n-butanol Production (PhD Thesis). TU Dortmund University, Dortmund.

Rühl, J., Hein, E.M., Hayen, H., Schmid, A., Blank, L.M., 2012. The

glycerophospholipid inventory of Pseudomonas putida is conserved between strains and enables growth condition-related alterations. Microb. Biotechnol. 5 (1), 45–58.
Sambrook, J., Maniatis, T., Fritsch, E.F., 1989. Molecular Cloning: A Laboratory Manual, 2nd ed Cold Spring Harbor Laboratory Press, Cold Spring Harbor, NY.
Scriba, P., Holzer, H., 1961. Gewinnung von alpha-Hydroxyathyl-2-thiaminpyrophosphat mit Pyruvatoxydase aus Schweineherzmuskel. Biochem. Z. 334 (5), 473–486.
Silva-Rocha, R., Martinez-Garcia, E., Calles, B., Chavarria, M., Arce-Rodriguez, A., de las Heras, A., Paez-Espino, A.D., Durante-Rodriguez, G., Kim, J., Nikel, P.I., Platero, R., de Lorenzo, V., 2013. The Standard European Vector Architecture (SEVA): a coherent platform for the analysis and deployment of complex prokaryotic phenotypes. Nucleic Acids Res 41 (D1), D666–D675.
Stephanopoulos, G.N., Aristidou, A.A., Nielsen, J., 1998. Metabolic Engineering – Principles and Methodologies. Academic Press, San Diego.
Sudarsan, S., Dethlefsen, S., Blank, L.M., Siemann-Herzberg, M., Schmid, A., 2014. The functional structure of central carbon metabolism in Pseudomonas putida KT2440. Appl. Environ. *Microbiol.* 80 (17), 5292–5303.
Tiso, T., Wierckx, N.J.P., Blank, L.M., 2015. Non-pathogenic Pseudomonas as Platform for Industrial Biocatalysis. In: Grunwald, P. (Ed.), Industrial Biocatalysis. Pan Stanford, Singapore, pp. 323–372.
de Weger, L.A., Jann, B., Jann, K., Lugtenberg, B., 1987. Lipopolysaccharides of Pseudomonas spp. that stimulate plant growth: composition and use for strain identification. J. Bacteriol. 169 (4), 1441–1446.
Wierckx, N.J.P., Ballerstedt, H., Bont, J.A.Md, Wery, J., 2005. Engineering of solvent-tolerant Pseudomonas putida S12 for bioproduction of phenol from glucose. Appl. Environ. Microbiol. 71 (12), 8221–8227.
Wittgens, A., 2013. Konstruktion neuer Produktionsstämme für die heterologe Rhamnolipidsynthese in dem nicht-pathogenen Wirt Pseudomonas putida KT2440 (PhD Thesis). Ulm University, Ulm.
Wittgens, A., Tiso, T., Arndt, T.T., Wenk, P., Hemmerich, J., Müller, C., Wichmann, R., Küpper, B., Zwick, M., Wilhelm, S., Hausmann, R., Syldatk, C., Rosenau, F., Blank, L.M., 2011. Growth independent rhamnolipid production from glucose using the non-pathogenic Pseudomonas putida KT2440. Microb. Cell Fact. 10 (80).
Xavier, K.B., Martins, L.O., Peist, R., Kossmann, M., Boos, W., Santos, H., 1996. High-affinity maltose/trehalose transport system in the hyperthermophilic archaeon Thermococcus litoralis. J. Bacteriol. 178 (16), 4773–4777.
Zobel, S., Benedetti, I., Eisenbach, L., de Lorenzo, V., Wierckx, N.J.P., Blank, L.M., 2015. Tn7-based device for calibrated heterologous gene expression in Pseudomonas putida. ACS Synth. Biol.